Acceleration of Tuberculosis Treatment by Adjunctive Therapy with Verapamil as an Efflux Inhibitor

Shashank Gupta[1,2], Sandeep Tyagi[1], Deepak V. Almeida[1,3], Mariama C. Maiga[1,2], Nicole C. Ammerman[1,3], and William R. Bishai[1,2,3]

[1]Center for Tuberculosis Research, Department of Medicine, Johns Hopkins University, Baltimore, Maryland; [2]Howard Hughes Medical Institute, Chevy Chase, Maryland; and [3]KwaZulu-Natal Research Institute for Tuberculosis and HIV, Durban, South Africa

***Rationale*: A major priority in tuberculosis (TB) is to reduce effective treatment times and emergence of resistance. Recent studies in macrophages and zebrafish show that inhibition of mycobacterial efflux pumps with verapamil reduces the bacterial drug tolerance and may enhance drug efficacy.**

***Objectives*: Using mice, a mammalian model known to predict human treatment responses, and selecting conservative human bioequivalent doses, we tested verapamil as an adjunctive drug together with standard TB chemotherapy. As verapamil is a substrate for CYP3A4, which is induced by rifampin, we evaluated the pharmacokinetic/pharmacodynamic relationships of verapamil and rifampin coadministration in mice.**

***Methods*: Using doses that achieve human bioequivalent levels matched to those of standard verapamil, but lower than those of extended release verapamil, we evaluated the activity of verapamil added to standard chemotherapy in both C3HeB/FeJ (which produce necrotic granulomas) and the wild-type background C3H/HeJ mouse strains. Relapse rates were assessed after 16, 20, and 24 weeks of treatment in mice.**

***Measurements and Main Results*: We determined that a dose adjustment of verapamil by 1.5-fold is required to compensate for concurrent use of rifampin during TB treatment. We found that standard TB chemotherapy plus verapamil accelerates bacterial clearance in C3HeB/FeJ mice with near sterilization, and significantly lowers relapse rates in just 4 months of treatment when compared with mice receiving standard therapy alone.**

***Conclusions*: These data demonstrate treatment shortening by verapamil adjunctive therapy in mice, and strongly support further study of verapamil and other efflux pump inhibitors in human TB.**

Keywords: human equivalent doses; verapamil; efflux; *Mycobacterium tuberculosis*

Tuberculosis (TB), a disease affecting millions of people worldwide, requires treatment of patients with multiple drugs for several months. The complexity and length of therapy has led to the emergence of extensively drug-resistant *Mycobacterium tuberculosis*, which poses a global threat (1). The limited number of new antimicrobials in the TB drug development pipeline further emphasizes the need for fresh approaches in TB therapy. Repurposing existing approved drugs that may serve as treatment-shortening adjuvants is a promising and relatively efficient approach (2). Efflux pump inhibitors (EPIs) are potential agents in this category, and there have been initial promising reports for licensed agents, such as verapamil, reserpine, and piperine (3).

Recently, Adams and colleagues (4) showed that the bacterial efflux pump–encoding gene, *Rv1258c* promotes intracellular bacterial survival, and may mediate drug tolerance. Addition of verapamil reduced tolerance to rifampin in both *M. tuberculosis* and *Mycobacterium marinum*, and incubation of *M. marinum*–infected macrophages with verapamil reduced intracellular bacterial growth. When verapamil was added to isoniazid- and rifampin-treated *M. marinum*–infected macrophages, it restored antibiotic killing by reducing tolerance by more than twofold. This implies that verapamil may play a role in increasing the efficacy of existing antitubercular therapy.

Many of the EPIs like verapamil and reserpine have been shown to have an effect on drug-resistant *M. tuberculosis in vitro*. Reserpine is an ATP-dependent EPI that is shown to increase intracellular concentrations of ciprofloxacin and enhances susceptibility of some clinical isolates of *M. tuberculosis* (5). Reserpine also decreases the effective minimum inhibitory concentration (MIC) of linezolid both in drug-susceptible and -resistant *M. tuberculosis* strains. Verapamil inhibits *M. tuberculosis* efflux pumps in a calcium channel–independent manner. Interestingly, it has been shown previously that blocking calcium channels *in vivo* in *M. tuberculosis*–infected mice using specific antibodies significantly reduced bacterial loads (6). Induction of efflux pump expression or mutations enhancing pump activity may explain the newly attained multidrug resistance and tolerance induced by antimicrobial drug exposure (7–12). Furthermore, several mycobacterial efflux pumps, including Rv1258c, and their regulators are induced during macrophage infection (10, 13–18). Several of the EPIs enhance the activity of antimycobacterial drugs on drug-resistant *M. tuberculosis in vitro* and *in vivo*; these include the currently approved pump inhibitors, verapamil, reserpine, and thioridazine (3).

AT A GLANCE COMMENTARY

Scientific Knowledge on the Subject

Recent work has shown that, upon macrophage infection, *Mycobacterium tuberculosis* becomes tolerant to antitubercular drugs in a bacterial efflux pump–mediated process.

What This Study Adds to the Field

Our findings indicate that the addition of verapamil accelerates both the bactericidal and the sterilizing activity of standard tuberculosis treatment in an animal model.

(*Received in original form April 5, 2013; accepted in final form June 26, 2013*)

Supported by National Institute of Allergy and Infectious Diseases grants AI 079590, 037856, and 036973 and by the Howard Hughes Medical Institute.

Author Contributions: Conception and design: S.G. and W.R.B. Acquisition of data: S.G., S.T., D.V.A., and M.C.M. Analysis and interpretation: S.G., S.T., D.V.A., and N.C.A. Drafting the manuscript for important intellectual content: S.G. and W.R.B.

Correspondence and requests for reprints should be addressed to William Bishai, M.D., Ph.D., 1550 Orleans Street, Room 108, Baltimore, MD 21231-1001. E-mail: wbishai@jhmi.edu

This article has an online supplement, which is accessible from this issue's table of contents at www.atsjournals.org

Am J Respir Crit Care Med Vol 188, Iss. 5, pp 600–607, Sep 1, 2013

Originally Published in Press as DOI: 10.1164/rccm.201304-0650OC on June 27, 2013
Internet address: www.atsjournals.org

Here, we explored the activity of verapamil in the mouse model, a model representative of chemotherapy of human TB, in which verapamil (V) is added to the standard 6-month daily regimen (2 mo of isoniazid [H], rifampin [R], and pyrazinamide [Z] followed with 4 mo of isoniazid and rifampin). The study was conducted in two different strains of mice—namely, C3H/HeJ and C3HeB/FeJ (commonly referred to in the literature as Kramnik mice). C3H/HeJ is a wild-type mouse strain commonly used for *M. tuberculosis* infection models. C3HeB/FeJ mice, which are derived from C3H mice, are of interest because, upon *M. tuberculosis* infection, they show more abundant tissue destruction in the lungs than C3H/HeJ mice (19). Indeed, *M. tuberculosis*–infected C3HeB/FeJ mice display lung granulomas with prominent necrotic areas of degenerating cells and dense infiltrates of neutrophils, which more closely resemble human granulomas than do the lesions of C3H/HeJ mice. We chose to do the study in C3HeB/FeJ mice, because this strain develops large, granuloma-like lesions, which are likely to harbor higher numbers of drug-tolerant bacteria akin to those studied by Adams and colleagues (4). Endpoints for our study were lung bacterial cfu counts, gross pathology, and histopathology. We also calculated the proportion of mice with culture-positive relapse 3 months after the completion of 4, 5, and 6 months of the indicated drug regimen.

METHODS

Animals

Approximately 6-week-old female C3H/HeJ and C3HeB/FeJ mice were purchased from The Jackson Laboratory (Bar Harbor, ME). Infected mice were maintained in an animal biosafety level 3 laboratory at all times. The mice used in the pharmacokinetic studies were housed in a pathogen-free environment.

Bacterial and Cell Culture Stocks

M. tuberculosis H37Rv passaged in mice was obtained from the Johns Hopkins Center for Tuberculosis Research stocks (Johns Hopkins Center for Tuberculosis Research, Baltimore, MD). For preparation for infections, the mycobacteria was grown to an optical density at 600 nm of approximately 1.0 in 7H9 Middlebrook liquid medium supplemented with oleic acid-albumin-dextrose-catalase (Becton Dickinson, Sparks, MD), 0.5% glycerol, and 0.05% Tween-80 (Sigma, St. Louis, MO).

Pharmacokinetics of Verapamil in Mouse

Single-dose serum pharmacokinetic profiles for verapamil were determined at a range of doses in uninfected C3H/HeJ mice. Three animals were killed at each time point ranging from 0 to 24 hours after the verapamil oral dose. Drug concentrations in mouse serum were determined by validated liquid chromatography–mass spectrometry assays, and pharmacokinetic relationships were evaluated from these data (20, 21). The assay was found to be linear over the whole calibration span ($r = 0.99921$). The limit of quantitation was fulfilled by the lowest point of the calibration curve (1 nM). Intra- and interday precision was less than 10%, and the accuracy varied between 98.4 and 108.7%. For steady-state verapamil pharmacokinetics, C3H/HeJ mice were administered rifampin (10 mg/kg) or rifabutin (10 mg/kg) orally for 10 days to induce the metabolizing enzyme CYP3A. Verapamil was administered orally, and three animals were killed at each time point, ranging from 0 to 8 hours, to measure verapamil concentrations in mouse serum by validated liquid chromatography–mass spectrometry assays.

Aerosol Infection Procedure

Aerosol infections were performed with *M. tuberculosis* H37Rv diluted appropriately to achieve the desired inoculum using the Glas-col Inhalation Exposure System (Terre Haute, IN) in three consecutive runs. All animal procedures were approved by the Johns Hopkins University Animal Care and Use Committee. For every infection, three mice were killed the following day to determine the Day-1 lung implantation. Lungs were dissected and homogenized in phosphate-buffered saline (PBS). The lung homogenates were then serially diluted and plated in duplicate on selective 7H11 agar plates (Fisher Scientific, Suwanee, GA); plates were incubated for 3 weeks at 37°C, and colonies were counted.

Drug Preparation and Administration

Isoniazid, rifampin, pyrazinamide, and verapamil were purchased from Sigma (St. Louis, MO). Isoniazid (10 mg/kg), rifampin (10 mg/kg), and pyrazinamide (150 mg/kg), with or without verapamil (9.4 mg/kg), were administered to mice by oral gavage daily for 5 d/wk. After the first 2 months of chemotherapy, pyrazinamide was discontinued from the regimen. Stock solutions were prepared weekly using distilled water and stored at 4°C (22). Drug solutions were prepared such that the desired concentration would be delivered in a 0.2-ml total volume. Rifampin was given 1 hour after administration of other drugs to avoid an adverse pharmacokinetic interaction (23).

Assessment of Treatment Efficacy

Baseline lung $\log_{10}$ cfu counts were assessed the day after aerosol infection and at treatment initiation. Treatment efficacy was assessed by comparing lung $\log_{10}$ cfu counts determined at specific time points during treatment. At the appropriate time points, five mice per group were killed. Total body weight was recorded, and then lungs were dissected and weighed. The lungs were kept in PBS for 24 hours at 4°C and then examined for gross pathology. Lung samples were homogenized and serially diluted in PBS and plated on selective 7H11 agar plates. cfu were counted after 3 weeks of incubation at 37°C.

Relapse Rates after Treatment

We compared the proportion of mice with culture-positive relapse 3 months after completion of treatment. Mice were considered to be culture positive if 1 or more cfu counts were identified after plating the entire lung homogenate. The proportion of mice with culture-positive relapse was determined after 16, 20, and 24 weeks of treatment.

Statistical Analysis

Lung cfu counts were $\log_{10}$ transformed before analysis. Mean cfu counts were compared using Student's *t* test. The proportions of mice relapsing were compared using Fisher's exact test (STATA 8.2; StataCorp, College Station, TX). All measures of statistical variation are expressed as ±SD.

RESULTS

Pharmacokinetic Studies and Dose Selection for Verapamil Treatment

Several formulations of verapamil are clinically available (*see* Table E4 in the online supplement). Although 200 mg of extended-release verapamil achieves an area under the concentration curve (AUC) of over 1,000 ng·h/ml over 24 hours, 40 mg of standard verapamil gives an AUC of approximately 234 ng·h/ml over 8 hours. Assuming that future clinical evaluation of verapamil for TB would be conducted using conservative doses, we sought to employ mouse dosing in our experiments that would achieve an AUC of approximately 250 ng·h/ml, the human bioequivalent of 40 mg daily of standard verapamil. We evaluated the pharmacokinetic interactions of verapamil and rifampin in the mouse model and compared it to the 40-mg human dose. Concentration time profiles were established for verapamil administered by oral gavage in mice as a single drug or in combination (Figure 1A). Standard pharmacokinetic parameters were calculated from the profiles of three animals at each time point (Table E1A). These were compared with the AUC achieved with human doses to model human dosing in mice. Verapamil (6.25 mg/kg) had an AUC(0–8)

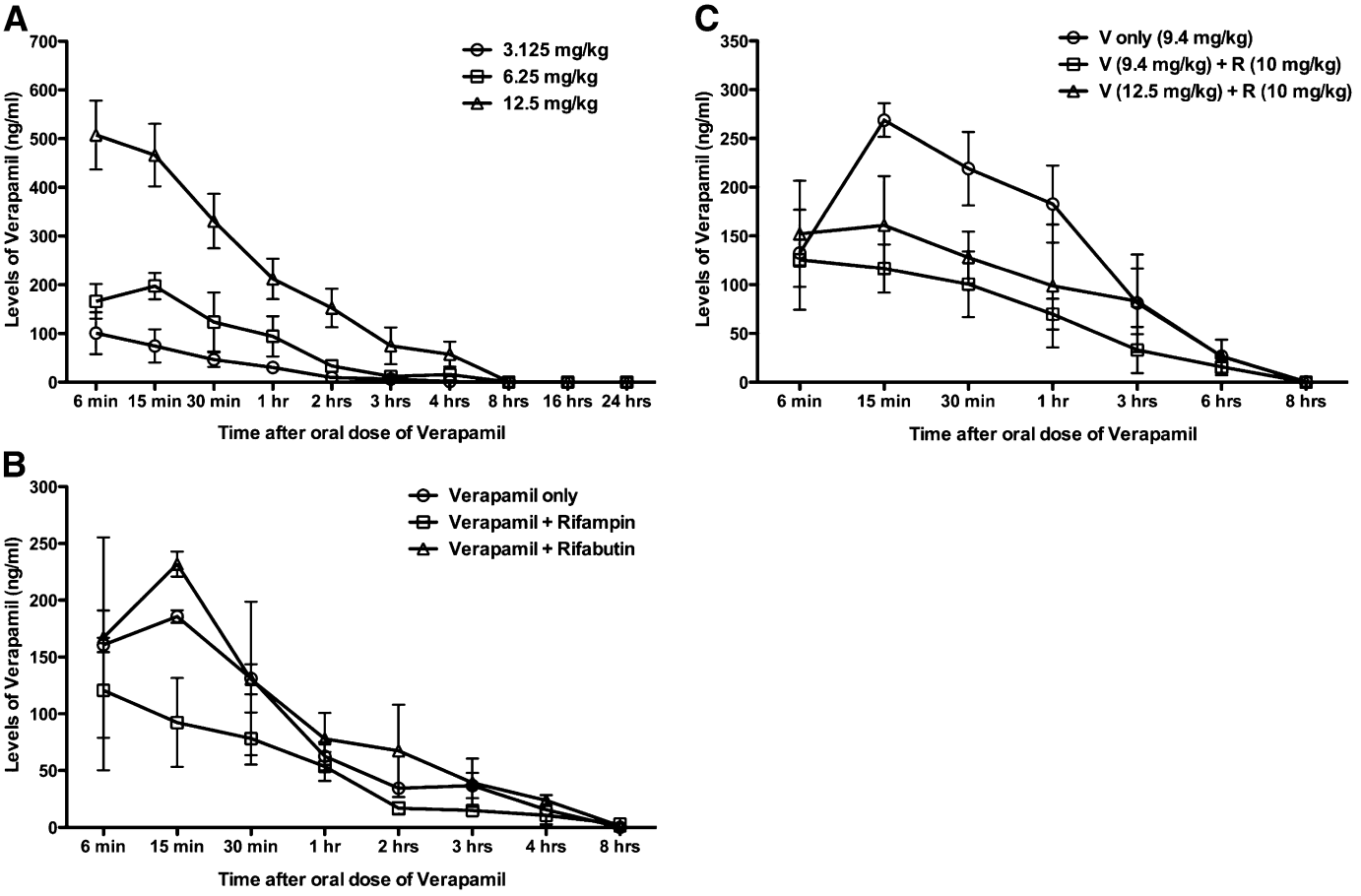

Figure 1. Pharmacokinetic parameters of verapamil in the mouse model. (*A*) Groups of mice were given a single dose of verapamil orally at different concentrations. Blood samples were withdrawn by cardiac puncture at indicated time points after oral administration. The levels of verapamil were measured by liquid chromatography–mass spectrometry (LC-MS). (*B*) Mice were given the drugs orally at doses of verapamil of 6.25 mg/kg, rifampin of 10 mg/kg, and rifabutin of 10 mg/kg. Rifampin and rifabutin were given daily to mice for 10 days to reach a steady-state level of metabolizing enzyme, CYP3A. Blood samples were withdrawn by cardiac puncture at indicated time points after oral administration of drugs. (*C*) Mice were given the drugs orally at indicated doses of verapamil (V) and rifampin (R). The levels of verapamil were measured by LC-MS in the blood samples. Values are expressed as average (±SD).

of 255 ng·h/ml, which is close to the human AUC(0–8) of 234 ng·h/ml and is a dose used in previous studies (9, 24).

Verapamil has a known drug–drug interaction with rifampin, due to the fact that rifampin is a potent inducer of the CYP3A4 enzyme system that metabolizes verapamil. In humans, rifampin causes up to a 10-fold reduction in plasma levels of orally administered verapamil (25, 26). To assess the nature of this interaction in mice, we measured mouse plasma verapamil levels after steady-state induction by rifampin for 10 days. When rifampin was administered orally, we found that the levels of verapamil were reduced, but to a lesser extent than that reported in humans. With rifabutin (a rifamycin that is known to be a poor liver enzyme inducer), the levels of verapamil in mouse plasma remained stable (Figure 1B, Table E1B). Because rifampin is a standard anti-TB drug used globally and is the rifamycin of choice, we used rifampin in our experiments with an appropriate adjustment in the verapamil dose.

To identify the correct dose adjustment for verapamil when coadministered with rifampin in mice, we sought the verapamil dose that achieved the same AUC as is observed in humans. Increasing the verapamil dose by 50% (from 6.25 to 9.4 mg/kg) when coadministered with rifampin achieved the same AUC (Table E1C) as 6.25 mg/kg of verapamil only in mice (Figure 1C), and hence the 9.4 mg/kg verapamil dose was used in subsequent studies.

Rapid Clearance of Mycobacteria from Lungs during the First 2 Months of Treatment with Verapamil

We first assessed the possibility that verapamil has direct antibacterial activity against *M. tuberculosis in vitro*. Using the microplate Alamar blue assay, we found that verapamil has an MIC of 200 μg/ml against *M. tuberculosis* H37Rv. In the presence of 100 μg/ml of verapamil (50% of the MIC), we found that the intrabacterial levels of rifampin were increased at least twofold in 2 hours, presumably due to a direct effect on bacterial efflux pumps by verapamil (Figure E1).

Next, we evaluated the potency of verapamil when added to standard TB chemotherapy (Std-Tx) in the acute mouse model of TB after aerosol infection in which high cfu counts are implanted ($\sim 10^4$ cfu) and antimicrobial therapy is initiated 2 weeks later. We conducted the experiment in C3HeB/FeJ (Kramnik) mice, which develop large necrotic lung granulomas after infection with *M. tuberculosis*, and used the wild-type

C3H/HeJ mice as the control group. Each of the two strains of mice were infected with *M. tuberculosis* H37Rv and treated daily with verapamil plus Std-Tx (2HRZV-4HRV) and Std-Tx (2HRZ-4HR) alone for 6 months (Table E2).

The initial cfu implantation the day after aerosol infection (Day −13) was 4.16 (±0.11) log units, and the cfu bacterial load at the start of the treatment (Day 0) was 7.51 (±0.10) log units. The C3HeB/FeJ mice formed well developed characteristic granulomas with central caseation (Figure 2A) in which abundant acid-fast bacilli could be seen within both the necrotic central region and in the peripheral rim of giant cells (Figure 2A). The lungs of both C3HeB/FeJ and C3H/HeJ mice harbored similar zones of chronic inflammation, with nests of foamy macrophages containing acid-fast bacilli (Figure E2). Gross pathology revealed that, as early as 4 weeks into treatment, C3HeB/FeJ mice receiving 4HRZV-2HRV had fewer visible lesions compared with those receiving 4HRZ-2HR (Figure 2B and Figures E3 and E4).

We determined quantitative lung cfu counts at 0, 2, 4, 8, 12, 16, 20, and 24 weeks of treatment (Figures 3A and 3B). The C3HeB/FeJ and the C3H/HeJ mouse strains showed similar cfu responses to Std-Tx, which were comparable to those seen with BALB/c mice (27). In C3HeB/FeJ mice, Std-Tx yielded a cfu decrease of 1.5 log units at 2 weeks, whereas the Std-Tx plus verapamil group gave quantitative cfu counts that were 0.32 log units lower (P value < 0.01). In C3HeB/FeJ mice, the lung cfu count difference between the Std-Tx and the Std-Tx plus verapamil groups continued to widen over the course of treatment, going from 0.84 to 0.87 to 1.15 log units at Weeks 4, 8, and 12, respectively (P value for the two treated groups is <0.001 for Weeks 8 and 12).

The lung cfu counts in C3H/HeJ mice also dropped by approximately 1.4 log units in the Std-Tx recipients during the first 2 weeks. Adding verapamil to Std-Tx had a modest effect at Week 2, with a further 0.24–log unit reduction. In contrast to C3HeB/FeJ mice, the cfu count difference between the Std-Tx and Std-Tx plus verapamil groups did not widen over the course of treatment in C3H/HeJ mice, with differences of only 0.19 log units at Week 4. We also measured a panel of cytokines from lung and spleen homogenates, but did not find any significant differences in the levels between the RHZ- and RHZV-treated groups.

Accelerated Culture Conversion in C3HeB/FeJ Mice Receiving Std-Tx plus Verapamil

At Month 4 of Std-Tx plus verapamil treatment, all C3HeB/FeJ mice were culture negative and remained so at Months 5 and 6, demonstrating a significant acceleration of culture conversion with the addition of verapamil to Std-Tx. In contrast, C3HeB/FeJ mice receiving Std-Tx alone had Month-4 cfu counts of 0.46 log units, and did not demonstrate complete culture conversion to negative until Month 6. Thus, verapamil led to a 2-month acceleration of culture conversion in C3HeB/FeJ mice. In the C3H/HeJ mouse group, verapamil also had a moderate beneficial effect at 3 months of treatment, with cfu counts 0.63 log units lower than in Std-Tx–alone recipients. At 4 months of Std-Tx plus verapamil treatment in C3H/HeJ mice, four of the five mice were culture negative, and one mouse had a total of 25 cfu counts in the whole lung, whereas, at Months 5 and 6, all C3H/HeJ mice receiving verapamil were culture negative. Hence, in C3H/HeJ mice, the addition of verapamil to Std-Tx accelerated culture conversion by 1 month (Figure 3B, Table E3).

Relapse Rates after Treatment Completion

To assess durable sterilization, we evaluated the 3-month relapse-free cure rates for all treatment groups. We held groups of mice after 4, 5, or 6 months of treatment for an additional 3 months without drug therapy, and then killed them to determine the fraction of mice showing any lung cfu. At the 4-month mark, C3HeB/FeJ mice receiving Std-Tx showed a 3-month drug-free relapse rate of 100%, whereas those receiving Std-Tx plus verapamil showed only 50% relapse ($P < 0.05$, Fisher's exact test). After 5 months of treatment, 20% of mice in the Std-Tx group had relapsed, whereas 0% of the Std-Tx plus verapamil mice had relapsed. After 6 months of treatment, both treatment groups of C3HeB/FeJ mice had a 3-month drug-free relapse rate of 0% (Figures 4A and 4C).

For C3H/HeJ mice, after 4 months of treatment, the 3-month drug-free relapse rate was 75% in the Std-Tx group and 63% in the Std-Tx plus verapamil group. After 5 months of treatment, it was 13% in the Std-Tx group and 0% in the Std-Tx plus verapamil group. Similar to C3HeB/FeJ mice, both treatment arms of

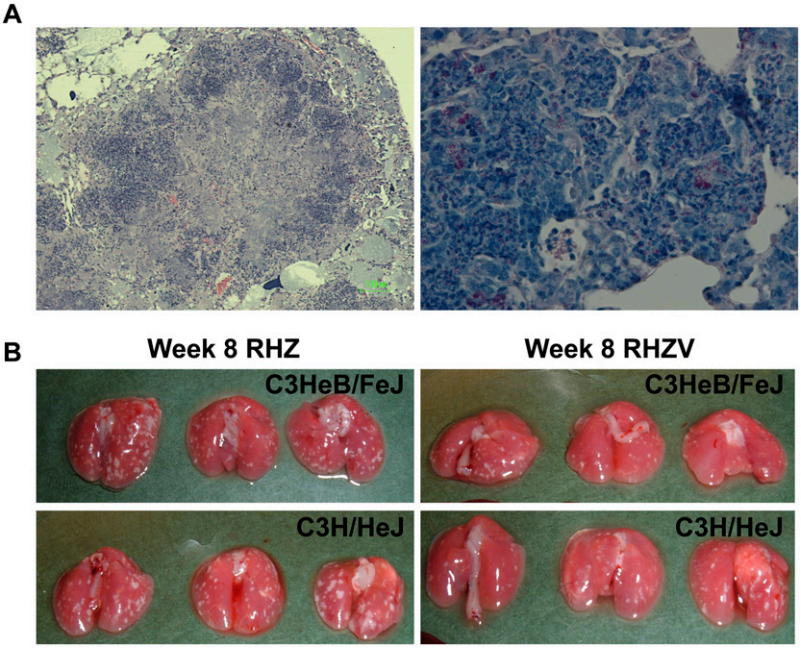

Figure 2. Adjunctive drug treatment with verapamil improves pathology of *Mycobacterium tuberculosis*–infected lungs. (*A*) Microscopic histopathology of lungs at 2 weeks of infection in C3HeB/FeJ mice. The *left panel* is hematoxylin and eosin staining (40×), and the *right panel* is acid fast staining for *M. tuberculosis* H37Rv (500×). (*B*) Gross lung pathology at 8 weeks of treatment in different groups, as indicated.

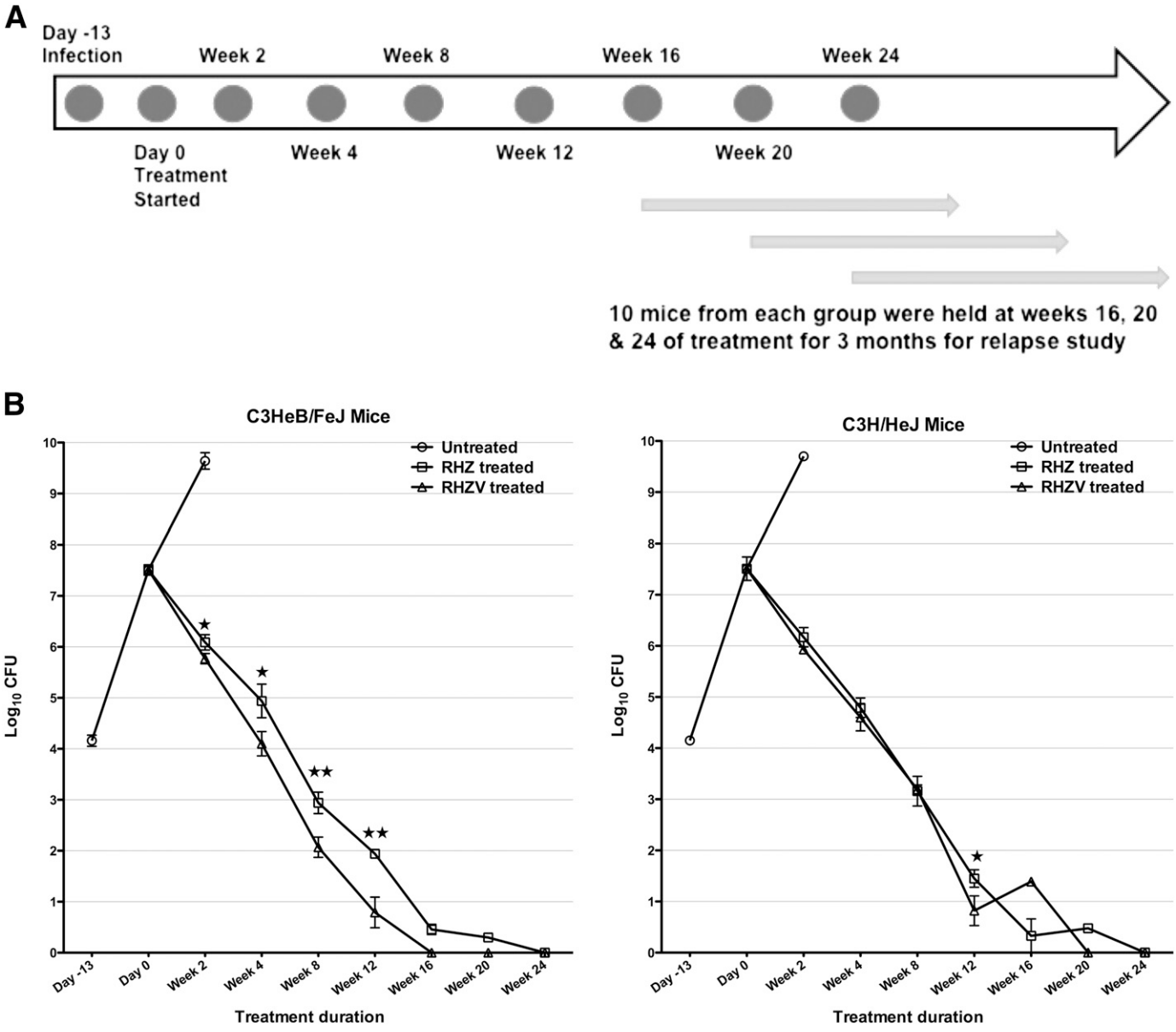

Figure 3. Adjunctive drug treatment with verapamil reduces bacterial counts during active disease. (*A*) Timeline and experimental scheme for the 9 months of the experiment. A total of 10 mice from each group were held at Weeks 16, 20, and 24 of treatment for an additional 3 months without any treatment for relapse study. (*B*) C3HeB/FeJ and C3H/HeJ mice were infected with Log_{10} 4.2 *Mycobacterium tuberculosis* H37Rv, and the treatment started at Day 14 after infection. The mice were treated with rifampin (R; 10 mg/kg), isoniazid (H; 10 mg/kg), pyrazinamide (Z; 150 mg/kg), and verapamil (V; 9.40 mg/kg) daily for 5 d/wk. The lungs were homogenized, diluted, and plated for cfu counts and expressed as Log_{10} cfu ($\pm$SD). $^{\star}P < 0.01$ and $^{\star\star}P < 0.001$ for RHZ versus RHZV groups.

the C3H/HeJ mice showed a 3-month drug-free relapse rate of 0% after 6 months of treatment (Figures 4B and 4C).

DISCUSSION

This is the first study showing the use of verapamil in the 6-month mouse model of TB chemotherapy. Using a daily dose of verapamil adjusted to give a conservative human bioequivalent AUC with appropriate adjustment for rifampin coadministration, we have shown that the addition of verapamil accelerates both the bactericidal activity of Std-Tx (lung cfu reduction of 1.15 log units at 12 wk) and the achievement of durable sterilization (2 mo acceleration). The bactericidal and sterilizing advantages occurred in C3HeB/FeJ mice, which develop necrotic granulomatous lesions, although we also observed more modest advantages of verapamil in wild-type C3H/HeJ mice with a lung cfu reduction of 0.63 log units and a 1-month acceleration of durable sterilization. Throughout, we used doses of anti-TB drugs known to be bioequivalent to human dosing, and before the long-term mouse study, we selected a conservative human bioequivalent dose of verapamil both alone and in the presence of rifampin, which is known to accelerate verapamil clearance.

The long duration of antibiotic treatment for *M. tuberculosis* treatment may be due to the microbe's entry into a nonreplicating (dormant) state in the host. The nonreplicating state probably renders *M. tuberculosis* phenotypically resistant to the antitubercular

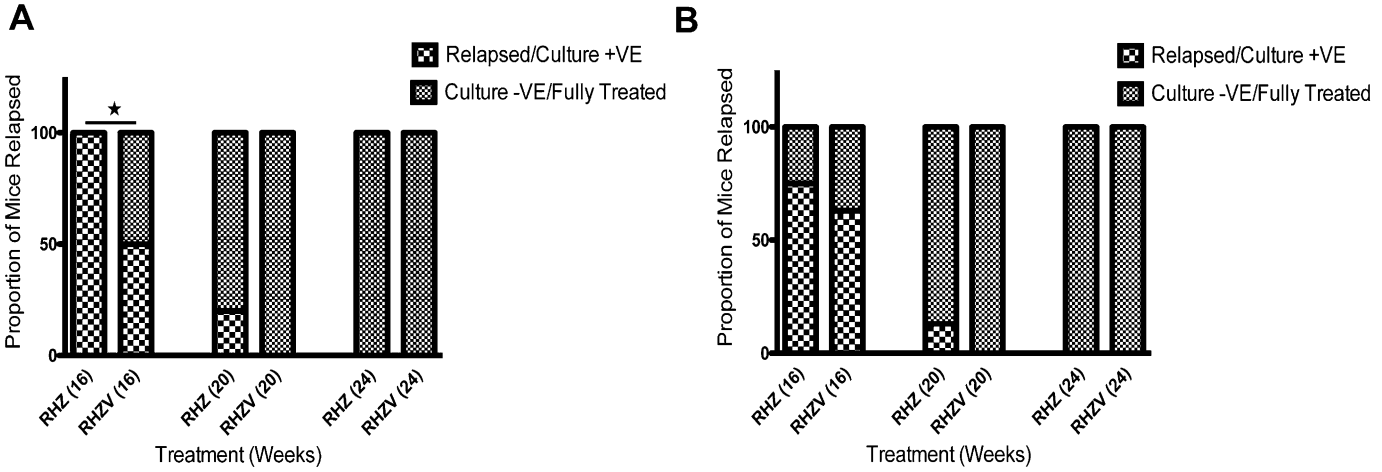

C

Treatment Groups	Percentage (proportion) of mice relapsing after treatment for:		
	16 Weeks	20 Weeks	24 Weeks
C3HeB/FeJ			
RHZ	100	20	0
RHZV	50	0	0
C3H/HeJ			
RHZ	75	13	0
RHZV	63	0	0

Figure 4. Reduction in relapse rates in C3HeB/FeJ mice by adjunctive drug treatment with verapamil. C3HeB/FeJ (*A*) and C3H/HeJ (*B*) mice were treated for the indicated time and then the treatment was discontinued for 3 months. Mice were then killed and whole lungs homogenized and plated, and the proportion of mice relapsed was estimated ($P < 0.05$ for rifampin + isoniazid + pyrazinamide [RHZ] vs. RHZ + verapamil [V] at 16 wk of treatment, Fisher's exact test). A total of 10 mice was used in the C3HeB/FeJ group, whereas 8 mice were used for C3H/HeJ strain. (*C*) The percentage of mice relapsing after the treatment in different groups was calculated and depicted in tabular format. −VE = negative; +VE = positive.

drugs (20, 28). Recent work has shown that *M. tuberculosis* dormant state may be due to tolerance to antitubercular drugs mediated by bacterial efflux pumps that are up-regulated upon bacterial entry into macrophages (4). Verapamil is known to inhibit tolerance and increase susceptibility to rifampin and isoniazid (4, 29). By inhibiting tolerance to these two key drugs, verapamil may accelerate *M. tuberculosis* clearance during active pulmonary TB by potentiating antibiotic killing. In addition, it has been shown that macrophage-induced *M. tuberculosis* tolerance persists after lysis of macrophages; this mechanism is potentially important for bacterial tolerance in the necrotic caseum, where bacilli may be extracellular (4). In addition to its potential role as an antimycobacterial agent, verapamil has been previously shown to block the acquisition of drug resistance in *Trypanosoma cruzi* and *Leishmania donovani* (30), and chloroquine resistance in *Plasmodium falciparum* (31).

Verapamil was recently shown to restore susceptibility toward first-line anti-TB drugs in mice infected with a multidrug-resistant *M. tuberculosis* strain (9). The authors infected the mice intratracheally and treated different groups of mice with or without verapamil for 2 months. Verapamil dosed at 6.25 mg/kg in combination with first-line anti-TB drugs (isoniazid, rifampin, pyrazinamide, and verapamil) reduced the mouse lung cfu counts by approximately 75% at 60 days after initiation of treatment when compared with a nontreated control group. Our study significantly extends this early observation by using the aerosol infection route (which better approximates natural infection), a validated drug-susceptible *M. tuberculosis* isolate (H37Rv), validated human doses of verapamil, which are at the low end of the clinically achievable spectrum in humans, and a 6-month treatment regimen, which, like human treatment, leads to durable sterilization after 6 months, but not sooner. In addition, before our mouse treatment study, we conducted a pharmacologic assessment of the rifampin–verapamil drug–drug interaction. Although it is known that concomitant rifampin administration lowers levels of orally administered verapamil by approximately 90% via induction of CYP3A4 in humans (25, 26, 32), the earlier 2-month mouse study with multidrug-resistant TB infection did not adjust the verapamil dosing for this interaction. Our pharmacologic assessment revealed that, in mice receiving steady-state rifampin, it is necessary to use a verapamil dose of 9.4 mg/kg to achieve a daily AUC equivalent to that achieved with 40 mg/d of verapamil in humans.

Rifampin, a potent inducer of the hepatic microsomal system, has been known to cause clinically important drug interactions. It induces CYP3A4, the predominant hepatic cytochrome P450 enzyme, which plays a critical role in detoxifying drugs. In humans, oral administration of rifampin with verapamil reduces the latter's levels by approximately 90% by induction of CYP3A4. We studied the drug–drug interactions in mice of verapamil with both rifampin and rifabutin, and determined the appropriate murine dose adjustment required for rifampin–verapamil coadministration. Although we considered an in-depth study of rifabutin (which does not require a verapamil dose adjustment)

instead of rifampin in the mouse model, we chose to use dose-adjusted rifampin in our experiments. Despite the advantage of rifabutin being a weak CYP3A4 inducer (confirmed by our mouse data), we opted for rifampin, because it is the preferred rifamycin for anti-TB treatment in humans, has fewer side effects, and is less expensive. Because data on steady-state rifamycin–verapamil interactions in humans are limited, additional clinical studies are warranted to address the issue of dose adjustment of verapamil when coadministered with rifampin or rifabutin in humans.

It is noteworthy that the optimal effect of verapamil was observed in C3HeB/FeJ mice rather than in the C3H/HeJ strain. C3HeB/FeJ mice are highly susceptible to *M. tuberculosis* infection, and develop necrotic granulomas in which the bacilli are exposed to hypoxic conditions (33, 34). In contrast, C3H/HeJ mice do not develop necrosis, and the majority of bacilli appear to reside intracellullarly by histologic assessment. Although the relative beneficial effect of verapamil on the standard TB treatment was apparent in both mouse strains, the magnitude of the effect was greater in the C3HeB/FeJ mice, which develop necrotic lesions, extracellular bacilli, and hypoxia. The benefit of verapamil in the presence of necrosis, extracellular bacilli, and hypoxia suggests that these factors are inducers for efflux pump expression and the persister phenotype. Tuberculous lesions in wild-type mice (BALB/c, C3H/HeJ, and C57BL/6) are not known to be hypoxic (34); hence, our results in C3H/HeJ mice are likely to extend to these other mouse strains. In contrast, nonhuman primates have granulomatous lung pathology with caseous necrosis resembling the human disease, and hence our results in C3HeB/FeJ may parallel verapamil's efficacy in these animals as well as humans.

The results and discussion presented here must be interpreted keeping in mind that we have measured the verapamil levels in mice using the C3H/HeJ strain. Although the TB drug metabolism in the C3HeB/FeJ mouse is unlikely to be significantly different from the C3H/HeJ mouse, this possibility cannot be ruled out. In addition, verapamil can inhibit P-glycoprotein–mediated clearance of rifampin and/or isoniazid, which can lead to altered serum concentrations of the two antitubercular drugs. Almeida and colleagues (35) have demonstrated the antagonism between isoniazid and the combination of rifampin–pyrazinamide, which increases with higher doses of isoniazid. In the context of this observation, the improved bactericidal activity of RHZV compared with RHZ in C3HeB/FeJ mice cannot be attributed to a verapamil-mediated elevation of isoniazid levels. Altered rifampin concentrations due to verapamil cannot be ruled out with the data available, and may be responsible, in part, for the accelerated bacterial clearance with RHZV.

This study provides data that a drug targeting bacterial efflux pumps during active TB can be effective in treatment of the disease. The mouse TB model with human bioequivalent doses of antitubercular drugs is a rigorous animal model for testing drug effectiveness for active TB, and has frequently formed the basis of human clinical trials. The successful use of verapamil as an adjunct drug for TB therapy in a mouse model provides a scientific framework for human studies of this treatment-shortening combination, and suggests that developing improved alternative EPIs will be helpful.

Author disclosures are available with the text of this article at www.atsjournals.org.

References

1. World Health Organization. Global tuberculosis control 2011. Geneva: WHO Press; 2011.
2. Paige C, Bishai WR. Penitentiary or penthouse condo: the tuberculous granuloma from the microbe's point of view. *Cell Microbiol* 2010;12: 301–309.
3. Li XZ, Nikaido H. Efflux-mediated drug resistance in bacteria: an update. *Drugs* 2009;69:1555–1623.
4. Adams KN, Takaki K, Connolly LE, Wiedenhoft H, Winglee K, Humbert O, Edelstein PH, Cosma CL, Ramakrishnan L. Drug tolerance in replicating mycobacteria mediated by a macrophage-induced efflux mechanism. *Cell* 2011;145:39–53.
5. Huang TSKC, Wang HM, Yan BS, Huang SP, Chen YS, Lee SSJ, Syu WJ. Inhibition of the *Mycobacterium tuberculosis* reserpine–sensitive efflux pump augments intracellular concentrations of ciprofloxacin and enhances susceptibility of some clinical isolates. *J Formos Med Assoc* (In press)
6. Gupta S, Salam N, Srivastava V, Singla R, Behera D, Khayyam KU, Korde R, Malhotra P, Saxena R, Natarajan K. Voltage gated calcium channels negatively regulate protective immunity to mycobacterium tuberculosis. *PLoS One* 2009;4:e5305.
7. De Rossi E, Ainsa JA, Riccardi G. Role of mycobacterial efflux transporters in drug resistance: an unresolved question. *FEMS Microbiol Rev* 2006;30: 36–52.
8. Gupta AK, Katoch VM, Chauhan DS, Sharma R, Singh M, Venkatesan K, Sharma VD. Microarray analysis of efflux pump genes in multidrug-resistant *Mycobacterium tuberculosis* during stress induced by common anti-tuberculous drugs. *Microb Drug Resist* 2010;16:21–28.
9. Louw GE, Warren RM, Gey van Pittius NC, Leon R, Jimenez A, Hernandez-Pando R, McEvoy CR, Grobbelaar M, Murray M, van Helden PD, *et al*. Rifampicin reduces susceptibility to ofloxacin in rifampicin-resistant *Mycobacterium tuberculosis* through efflux. *Am J Respir Crit Care Med* 2011;184:269–276.
10. Morris RP, Nguyen L, Gatfield J, Visconti K, Nguyen K, Schnappinger D, Ehrt S, Liu Y, Heifets L, Pieters J, *et al*. Ancestral antibiotic resistance in *Mycobacterium tuberculosis*. *Proc Natl Acad Sci USA* 2005;102:12200–12205.
11. Viveiros M, Portugal I, Bettencourt R, Victor TC, Jordaan AM, Leandro C, Ordway D, Amaral L. Isoniazid-induced transient high-level resistance in *Mycobacterium tuberculosis*. *Antimicrob Agents Chemother* 2002;46:2804–2810.
12. Piddock LJ. Clinically relevant chromosomally encoded multidrug resistance efflux pumps in bacteria. *Clin Microbiol Rev* 2006;19:382–402.
13. Fontan PA, Aris V, Alvarez ME, Ghanny S, Cheng J, Soteropoulos P, Trevani A, Pine R, Smith I. *Mycobacterium tuberculosis* sigma factor E regulon modulates the host inflammatory response. *J Infect Dis* 2008;198:877–885.
14. Nguyen L, Thompson CJ. Foundations of antibiotic resistance in bacterial physiology: the mycobacterial paradigm. *Trends Microbiol* 2006;14: 304–312.
15. Ramon-Garcia S, Martin C, Thompson CJ, Ainsa JA. Role of the *Mycobacterium tuberculosis* p55 efflux pump in intrinsic drug resistance, oxidative stress responses, and growth. *Antimicrob Agents Chemother* 2009;53:3675–3682.
16. Rohde KH, Abramovitch RB, Russell DG. *Mycobacterium tuberculosis* invasion of macrophages: linking bacterial gene expression to environmental cues. *Cell Host Microbe* 2007;2:352–364.
17. Schnappinger D, Ehrt S, Voskuil MI, Liu Y, Mangan JA, Monahan IM, Dolganov G, Efron B, Butcher PD, Nathan C, *et al*. Transcriptional adaptation of *Mycobacterium tuberculosis* within macrophages: insights into the phagosomal environment. *J Exp Med* 2003;198:693–704.
18. Zahner D, Zhou X, Chancey ST, Pohl J, Shafer WM, Stephens DS. Human antimicrobial peptide LL-37 induces MefE/Mel–mediated macrolide resistance in *Streptococcus pneumoniae*. *Antimicrob Agents Chemother* 2010;54:3516–3519.
19. Kamath AB, Alt J, Debbabi H, Behar SM. Toll-like receptor 4–defective C3H/HeJ mice are not more susceptible than other C3H substrains to infection with *Mycobacterium tuberculosis*. *Infect Immun* 2003;71:4112–4118.
20. Chytil L, Strauch B, Cvacka J, Maresova V, Widimsky J Jr, Holaj R, Slanar O. Determination of doxazosin and verapamil in human serum by fast LC-MS/MS: application to document non-compliance of patients. *J Chromatogr B Analyt Technol Biomed Life Sci* 2010;878:3167–3173.
21. Lee YS, Yoon JN, Yoon IS, Lee MG, Kang HE. Pharmacokinetics of verapamil and its metabolite norverapamil in rats with hyperlipidaemia induced by poloxamer 407. *Xenobiotica* 2012;42:766–774.
22. Grosset J, Almeida D, Converse PJ, Tyagi S, Li SY, Ammerman NC, Pym AS, Wallengren K, Hafner R, Lalloo U, *et al*. Modeling early bactericidal activity in murine tuberculosis provides insights into the

activity of isoniazid and pyrazinamide. *Proc Natl Acad Sci USA* 2012; 109:15001–15005.
23. Dhillon J, Dickinson JM, Sole K, Mitchison DA. Preventive chemotherapy of tuberculosis in Cornell model mice with combinations of rifampin, isoniazid, and pyrazinamide. *Antimicrob Agents Chemother* 1996;40: 552–555.
24. John DN, Fort S, Lewis MJ, Luscombe DK. Pharmacokinetics and pharmacodynamics of verapamil following sublingual and oral administration to healthy volunteers. *Br J Clin Pharmacol* 1992;33:623–627.
25. Barbarash RA. Verapamil–rifampin interaction. *Drug Intell Clin Pharm* 1985;19:559–560.
26. Barbarash RA, Bauman JL, Fischer JH, Kondos GT, Batenhorst RL. Near-total reduction in verapamil bioavailability by rifampin: electrocardiographic correlates. *Chest* 1988;94:954–959.
27. Maiga M, Agarwal N, Ammerman NC, Gupta R, Guo H, Maiga MC, Lun S, Bishai WR. Successful shortening of tuberculosis treatment using adjuvant host-directed therapy with FDA-approved phosphodiesterase inhibitors in the mouse model. *PLoS ONE* 2012;7:e30749.
28. Lecoeur HF, Truffot-Pernot C, Grosset JH. Experimental short-course preventive therapy of tuberculosis with rifampin and pyrazinamide. *Am Rev Respir Dis* 1989;140:1189–1193.
29. Machado D, Couto I, Perdigao J, Rodrigues L, Portugal I, Baptista P, Veigas B, Amaral L, Viveiros M. Contribution of efflux to the emergence of isoniazid and multidrug resistance in *Mycobacterium tuberculosis*. *PLoS ONE* 2012;7:e34538.
30. Neal RA, van Bueren J, McCoy NG, Iwobi M. Reversal of drug resistance in *Trypanosoma cruzi* and *Leishmania donovani* by verapamil. *Trans R Soc Trop Med Hyg* 1989;83:197–198.
31. Martin SK, Oduola AM, Milhous WK. Reversal of chloroquine resistance in plasmodium falciparum by verapamil. *Science* 1987;235:899–901.
32. Mooy J, Böhm R, van Baak M, van Kemenade J, vd Vet A, Rahn KH. The influence of antituberculosis drugs on the plasma level of verapamil. *Eur J Clin Pharmacol* 1987;32:107–109.
33. Davis SL, Nuermberger EL, Um PK, Vidal C, Jedynak B, Pomper MG, Bishai WR, Jain SK. Noninvasive pulmonary [^{18}F]-2-fluoro-deoxy-d-glucose positron emission tomography correlates with bactericidal activity of tuberculosis drug treatment. *Antimicrob Agents Chemother* 2009;53:4879–4884.
34. Harper J, Skerry C, Davis SL, Tasneen R, Weir M, Kramnik I, Bishai WR, Pomper MG, Nuermberger EL, Jain SK. Mouse model of necrotic tuberculosis granulomas develops hypoxic lesions. *J Infect Dis* 2012; 205:595–602.
35. Almeida D, Nuermberger E, Tasneen R, Rosenthal I, Tyagi S, Williams K, Peloquin C, Grosset J. Paradoxical effect of isoniazid on the activity of rifampin–pyrazinamide combination in a mouse model of tuberculosis. *Antimicrob Agents Chemother* 2009;53:4178–4184.